Relationships between Nonlinear Normal Modes and Response to Random Inputs

Joseph D. Schoneman[*]
Matthew S. Allen[†]
Robert J. Kuether[‡]

Engineering Physics Department, University of Wisconsin-Madison, Madison, Wisconsin, 53706, USA

The ability to model nonlinear structures subject to random excitation is of key importance in designing hypersonic aircraft and other advanced aerospace vehicles. When a structure is linear, superposition can be used to construct its response to a known spectrum in terms of its linear modes. Superposition does not hold for a nonlinear system, but several works have shown how a system's dynamics can still be understood in terms of nonlinear modes. This work investigates the connection between a structure's undamped nonlinear normal modes and the spectrum of its response to high amplitude random forcing. Two examples are investigated, a spring-mass system and a clamped-clamped beam modeled within a geometrically nonlinear finite element package. In both cases, an intimate connection is observed between the smeared peaks in the spectrum of the response and the frequency-energy dependence of the nonlinear normal modes. For these two structures the dominant motion can be predicted using a single degree-of-freedom model that captures the frequency-energy dependence of the dominant mode or modes. This suggests that a reduced order model can be expected to give accurate results only if it is also capable of accurately predicting the frequency-energy dependence of the nonlinear modes that are in the frequency range of interest. On the other hand, the results also show cases where the result that one would expect based on linear superposition is not correct, especially in the vicinity of the higher frequency, more weakly excited modes.

I. Introduction

THE critical pressure loadings on the skin panels of concept hypersonic vehicles are random and broadband, resulting in response amplitudes that are so high that geometric nonlinearities cannot be neglected [1]. This phenomenon is also observed in a variety of thin-walled structures as the deflections approach the shell thickness. In general, the response of such a structure cannot be determined analytically, so the response to random loading must be found using numerical integration. This is extremely computationally expensive for realistic systems modeled with the finite element method, because long records are required to obtain a reasonable estimate of the response statistics. Even more importantly, these types of simulations do not provide design engineers with much insight regarding how changes to specific deformation modes of the structure might affect its response. Large scale models with nonlinearity can be reduced down to a low order representation using either reduced order models (ROMs), or nonlinear normal modes (NNMs). This work explores the connection between a structure's reduced order models, nonlinear normal modes, and response to random input in order to better develop simplified representations of complicated systems while maintaining accurate response predictions.

Nonlinear normal modes have received increased attention over the past several years. This work is primarily concerned with Rosenberg's definition [2] which was subsequently extended by Vakakis, Kerschen and others [3, 4] to define a NNM as a *not-necessarily synchronous periodic solution to the conservative nonlinear equations of motion*. One key feature of the NNM is the dependency of the system's natural frequency on response level. A common visual representation of this phenomenon is the frequency-energy plot, (FEP), on which a continuous

---

[*] Undergraduate Student, 538 Engineering Research Building, 1500 Engineering Drive, Madison, WI 53706-1609, schoneman@wisc.edu, AIAA Member.
[†] Associate Professor, 535 Engineering Research Building, 1500 Engineering Drive, Madison, WI 53706-1609, msallen@engr.wisc.edu, AIAA Lifetime Member.
[‡] Graduate Student, 534 Engineering Research Building, 1500 Engineering Drive, Madison, WI 53706-1609, rkuether@wisc.edu, AIAA Member.

backbone curve shows how the fundamental frequency of the NNM changes with increasing response amplitude (or energy). For example, a geometrically nonlinear structure that stiffens with increased deflection will exhibit NNMs which increase in frequency as the system energy increases.

The definition used here is also useful for describing the internal resonances that result as the underlying linear modes interact.[*] These internal resonances are observed in the frequency-energy space as branches off of the main backbone curve, and they occur as two or more of the modes in the system interact, typically when the ratio between their frequencies is rational (e.g. 3:1, 5:3, etc…). While many prior works have shown the effect that nonlinear stiffening has on the spectrum of the response (e.g. [1]), it is unclear what effect these internal resonances have and under what conditions they must be considered or may be neglected.

This work explores the connection between an NNM, the system model which produces them, and the structure's response to random forcing. In section II, the theory behind reduced order models and nonlinear normal modes is presented. Section III details an investigation of a two degree of freedom system with a cubic nonlinearity, while section IV investigates the response of a beam with geometric nonlinearity. Finally, section V offers discussion of the results and concludes the paper.

II. Theoretical Development

The equations of motion for an undamped, homogeneous, N degree-of-freedom nonlinear system can be written as

$$\mathbf{M}\ddot{\mathbf{x}} + \mathbf{K}\mathbf{x} + \mathbf{f}_{NL}(\mathbf{x}) = 0 \tag{1}$$

where $\mathbf{M}$ and $\mathbf{K}$ are the $N \times N$ linear mass and stiffness matrices, $\mathbf{f_{NL}(x)}$ is the $N \times 1$ nonlinear restoring force vector, and $\mathbf{x}$ is the displacement vector of the system. The structure's NNMs are defined as the periodic solutions to this conservative equation of motion. The motion of each coordinate is periodic with a common fundamental frequency, and each coordinate may also oscillate at higher harmonics as well. In the linear case, one finds the periodic solution by assuming $\mathbf{x} = \boldsymbol{\phi}\sin(\omega t)$ and inserting this into the equation of motion to obtain an eigenvalue problem that can be solved for the natural frequency, ω, and the mode shape, $\boldsymbol{\phi}$ of each of the N periodic responses that the linear system admits.

When the response amplitude is sufficiently low, N of the continuous branches of NNMs converge to the low energy linear modes of the system[†]. (A system may have more than N branches of NNMs. This will not be pursued here but it was discussed in [5, 6]. The NNMs considered here are only the fundamental NNMs, or those NNMs that emanate from the linear modes at low energy.) As the amplitude increases, the fundamental frequency and deformation shape will vary with increasing energy. An example of this is shown in Figure 1a, which gives the frequency-energy behavior of the two fundamental NNMs of a two-degree-of-freedom-system, which will be described in more detail in the following section. At the far left of the plot, each frequency-energy curve is flat; in this regime the NNM reduces to a linear mode of the structure and the mode shape would be well approximated by the linear mode shapes. As energy (or response amplitude) increases, the frequency of the NNMs begin to increase, revealing that the nonlinearity has a hardening effect on these nonlinear modes. It is interesting to note the excursion in the frequency-energy curve for the first NNM (near E=100 J, see [17] for a detailed view). At this energy level the first NNM branch of the structure has a frequency that is precisely 1/3 the frequency of the second and as a result the two NNMs can be thought to interact. The solutions in this region show significant participation of both the first and second linear mode shapes and the frequencies of both modes may be present. This is termed an internal resonance. In fact, an internal resonance is actually a point at which two branches of NNMs share a common solution, so the manifolds containing each branch of solutions intersect. While there may be many points in the frequency-energy plane where the NNM frequencies are integer related, internal resonances occur only at some of these depending on the shapes of the underlying manifolds.

The deformation shapes of a structure also change as energy increases. At low energy, the NNM shape is simply a periodic response of the linear structure deformed into one of its linear modes. At higher energy these become

_____

[*] In this paper we shall speak of linear and nonlinear modes and interactions between them because this type of description is helpful in understanding the physics of the system; we recognize that some may view this as a departure from the strict mathematical definitions of these terms.
[†] When a system is essentially nonlinear, some of the low energy modes may have zero fundamental frequencies.

multi-harmonic responses where each coordinate in the system may oscillate with many harmonics of the fundamental period.

The actual systems of interest are damped and the forces applied are a random function of time and space, so the equation of motion becomes more complicated. In this work the following form shall be assumed, in which the damping is light and linear, and the nonlinear forcing, $\mathbf{f}_{ext}(\mathbf{x},t)$, is a random function of time and position.

$$\mathbf{M}\ddot{\mathbf{x}} + \mathbf{C}\dot{\mathbf{x}} + \mathbf{K}\mathbf{x} + \mathbf{f}_{NL}(\mathbf{x}) = \mathbf{f}_{ext}(\mathbf{x},t) \tag{2}$$

The equation of motion above is a nonlinear, second order Stochastic Differential Equation (SDE) [7]. It should be noted that this equation has received considerable attention recently as various researchers have sought to design nonlinear energy harvesting systems for random vibration environments (see, e.g. [8]). The equation above can be written in a form known as the Fokker-Planck equation [9], and solutions to this can be found analytically for some low order systems, leading to further insights. Efficient solution strategies are also being developed for more general problems [9]. Cross and Worden recently studied a related approach for the SDOF version of this equation, revealing the level of approximation needed to capture different response phenomena, such as subharmonic peaks in the power spectra [10].

Little is known about how the response of a nonlinear system is related to its nonlinear modes, but there are a few limiting cases that are informative. All real systems have some degree of damping, so a persistent undamped NNM could only be observed in practice if a forcing was applied to exactly cancel the damping in the structure. This idea was developed by Peeters, Kerschen and Golinval in [11] with the aim of developing a modal testing method for nonlinear structures. Specifically, an NNM is obtained when

$$\mathbf{C}\dot{\mathbf{x}} = \mathbf{f}_{ext}(\mathbf{x},t) \tag{3}$$

and Peeters et al. used this to show that this can only occur if all harmonics of the forcing are 90 degrees out of phase with the response (or in phase with velocity). The force must also typically be applied at every node in the structure. While these conditions are not likely to be observed precisely in practice, this turns out to be an excellent approximation even when a single harmonic force is applied at only one node on the structure. This was also demonstrated in [12], where the authors found that higher harmonics do eventually become necessary to isolate an NNM at higher energies and especially near internal resonances.

Equation (3) can also be used to relate the forcing to the input amplitude. Nonlinear modes are periodic and so they are readily described in terms of a Fourier series

$$\mathbf{x} = \sum_{k=-\infty}^{\infty} \mathbf{X}_k e^{ik\omega_{\mathrm{NNM}}t} \tag{4}$$

and then Eq. (3) shows that the forcing, in conjunction with the damping, sets the amplitude $ik\omega_{\mathrm{NNM}}\mathbf{X}_k$ of the structure's velocity. In practice this must be solved iteratively together with the undamped equation of motion, eq. (1), to find a velocity pattern that both cancels the forcing and is an NNM. As the amplitude or energy in the structure increases, the fundamental frequency of the Fourier series, or the NNM frequency, changes, depending on the type of nonlinearity in the structure.

In this work we are concerned with random, broadband forces and so it is unlikely that Eq. (3) would be satisfied precisely in practice. However, the concept might still be helpful if Eq. (3) was satisfied in a statistical sense. More precisely, suppose that the structure were constrained so that it could respond only along a single NNM. This can be accomplished by constructing a reduced order model (ROM) that approximates the response of the structure in one of its NNMs using a one-degree-of-freedom model. One method that the authors have found to be quite effective is the Implicit Condensation and Expansion (ICE) method [13], and so this method will be explained briefly.

First, the conservative, linear equations of motion are obtained by neglecting the nonlinear force vector and damping matrix in Eq. (2). Using a classic modal transformation, these can be uncoupled by transforming from physical to modal coordinates,

$$\mathbf{x} = \mathbf{\Phi}\mathbf{q} \tag{5}$$

Where each column of $\mathbf{\Phi}$ is an eigenvector of the linear system, and $\mathbf{\Phi}$ is scaled such that

$$\mathbf{\Phi}^{\mathrm{T}}\mathbf{M}\mathbf{\Phi} = \mathbf{I}; \quad \mathbf{\Phi}^{\mathrm{T}}\mathbf{K}\mathbf{\Phi} = \mathbf{\Lambda} \tag{6}$$

with $\Lambda_{ii} = \omega_i^2$, and ω_i the ith natural frequency of the linear system. After pre-multiplying by $\mathbf{\Phi}^T$, the uncoupled equation of motion is

$$\ddot{\mathbf{q}} + \mathbf{\Lambda}\mathbf{q} = \mathbf{\Phi}^T\mathbf{f}_{ext}(t) \tag{7}$$

Energy dissipation can be accounted for in the system by introducing a modal damping ratio; the modal damping ratio for the ith mode is given by ζ_i. Additionally, the nonlinear restoring force can be re-introduced through the use of a nonlinear function of the modal coordinates, θ. Finally, a reduced set of m modes can be selected from the full set of N equations, reducing the system model to a low order system of nonlinear equations. The equation of motion for the rth mode then becomes

$$\ddot{q}_r + 2\zeta_r\omega_r\dot{q}_r + \omega_r^2 q_r + \theta_r(q_1, q_2, \ldots q_m) = \{\mathbf{\psi}\}_r^T \mathbf{f}_{ext}(t) \tag{8}$$

The only remaining concern is determination of the nonlinear modal force function $\theta_r(q_1, q_2, \ldots q_m)$, which is usually assumed to have the form of a polynomial in terms of the modal displacements. A polynomial with quadratic and cubic terms works very well for modeling the geometric nonlinearity of thin-walled beams and plates. Specifically, the nonlinear term takes the form,

$$\theta_r = \sum_{i=1}^{m}\sum_{j=1}^{m} B_r(i,j)q_i q_j + \sum_{i=1}^{m}\sum_{j=1}^{m}\sum_{k=1}^{m} A_r(i,j,k)q_i q_j q_k \tag{9}$$

For the cubic terms, a distinct three-dimensional coefficient array $A_r(i,j,k)$ is associated with each mode in the ROM, with a two-dimensional array for the quadratic terms. These coefficients can be found by applying a set of static loads to the structure and then solving a least squares problem [13]. Then one can compute the NNM(s) of the ROM using standard methods; in this work the authors employed the NNM continuation algorithm in [14], which is implemented in the Matlab® package "NNMcont", and can be found on Gaetan Kerschen's webpage[*].

In [15, 16] the authors found that, while different ROMs may give wildly differing estimates for the NNMs, a one-mode ICE ROM tends to give a very good estimate for the frequency-energy backbone curve of the mode of interest so long as the forces used to estimate the ROM are reasonable. In this work, these types of one-mode ROMs are useful since they allow one to study how the structure would behave if it had only one degree of freedom corresponding to that nonlinear mode.

III.   Motivation - Academic Test Case

The connection between a structure's nonlinear modes and its random response is readily illustrated using a simple example. The first system considered here is the simple 2DOF mass-spring system pictured in Figure 1b, which has the equations of motion given by,

$$\begin{bmatrix} m_1 & 0 \\ 0 & m_2 \end{bmatrix}\begin{Bmatrix} \ddot{x}_1 \\ \ddot{x}_2 \end{Bmatrix} + \beta\begin{bmatrix} k_1 & -k_1 \\ -k_1 & k_1 + k_2 \end{bmatrix}\begin{Bmatrix} \dot{x}_1 \\ \dot{x}_2 \end{Bmatrix} + \begin{bmatrix} k_1 & -k_1 \\ -k_1 & k_1 + k_2 \end{bmatrix}\begin{Bmatrix} x_1 \\ x_2 \end{Bmatrix} + \begin{Bmatrix} k_{nl,1}(x_1 - x_2)^3 \\ k_{nl,2}(x_2 - x_1)^3 \end{Bmatrix} = \begin{bmatrix} f_{ext}(t) \\ 0 \end{bmatrix} \tag{10}$$

The damping is stiffness-proportional with $\beta = 0.02$. In a previous work the authors used a similar system to explore methods to predict the nonlinear modes of an assembly from the nonlinear modes of the subcomponents [17]. Figure 1a shows the frequency-energy dependence of each of the system's fundamental nonlinear normal modes, for the case where the parameters of the system are: $m_1 = m_2 = 1$, $k_1 = 1$, $k_2 = 0.2$, and the cubic nonlinear spring coefficients are $k_{nl,1} = 0.5$ and $k_{nl,2} = $ 1e-5. This system is linearizable and the (constant with energy) natural frequencies of the corresponding linear modes are shown with dotted lines. The nonlinear mode shapes are not shown here, but it was observed that while the linear mode shapes of the system show similar motion of each of the masses (in phase and out of phase for the 1st and 2nd modes respectively), the motion of the system is dominated by only one or the other of the masses as energy increases. This phenomenon is referred to as localization and is common in certain classes of nonlinear systems.

Now, suppose that a random input is applied to the structure. This will impart a certain level of energy to each nonlinear mode of the structure (the nonlinear modes are not linearly independent so one cannot really say how much energy is in one mode or the other). Suppose that this input causes the total energy in the structure to be described by a probability distribution. As mentioned previously, one would hope to use the frequency-energy plot to predict how much each mode's response would be spread across a range of frequencies in the power spectrum.

---

[*] http://www.ltas-vis.ulg.ac.be/cmsms/index.php?page=kerschen (Accessed June 2013)
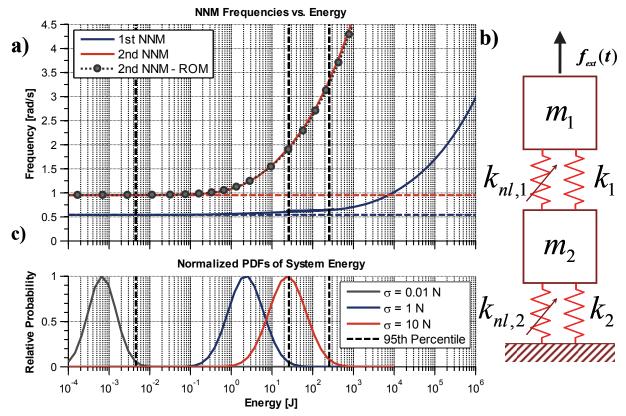
Figure 1. (a) Frequency-energy plot of the 2DOF system pictured in the schematic, (b). (c) Estimated log-normal probability distributions of the instantaneous energy level in each system.

These ideas were explored by applying a number of random broadband inputs to the system. The first mass was forced by a broadband, Gaussian random input, $f_{ext}(t)$, a zero-mean force with standard deviation σ. The response of the system to this input was computed using MATLAB's 'ode45' function, an adaptive 4th/5th order Runge-Kutta time integration routine. The input was generated using three different forcing levels, and, to facilitate the calculations, filtered with an 8th order, low-pass Butterworth filter with a cutoff frequency of 5 rad/s. Post-simulation, the instantaneous energy level of the system was computed at each instant in time and then that vector of energies was interrogated and found to resemble a log-normal distribution. MATLAB's statistical toolbox was then used to estimate the probability density function (PDF) of the energy for each case; the resulting PDFs (normalized to maximum values of one, for comparison) of the system energy are shown in Figure 1c, with the dashed vertical lines corresponding to the 95th percentile of each energy distribution. The three cases can be seen to correspond to low energy where the system is essentially linear (gray), medium energy where the nonlinearity begins to have a noticeable effect (blue), and very high nonlinearity (red). In the final case the second natural frequency has shifted by a factor of four or more and an internal resonance is present in the first NNM, near the 100 J energy level. Numerical values for the input and output of each case are given in Table 1.

Table 1: Details of the various simulated load cases for the 2DOF system

Input Std. Dev. σ [N]	Output 95th Percentile [J]
0.01	$4.56 \cdot 10^{-3}$
1	26.06
10	254.6

The power spectral densities of the mass responses were then computed and are shown in Figure 2. It is interesting to note how well the frequency content in each spectrum corresponds with the nonlinear mode frequencies and the energy in the system. For example, for the moderate excitation (blue lines in Figure 1c/Figure 2), 95% of the system energy lies below 26.06 J; at this point the first NNM frequency varies by only about 5% and the slope of the NNM backbone has barely begun to increase. Corresponding with these observations, the first peak in the autospectrum has not shifted or spread significantly compared to the low-amplitude input. In contrast, the second NNM features a significant frequency shift, and the backbone curve has a much higher slope at this level than the first NNM's. Examining the second peak of Figure 2, it is clear that the peak has shifted and spread considerably compared to the linear response. Similar comments could be made about the comparison when the system was excited at higher and lower energies. It is somewhat surprising that the random response of a system such as this, which can potentially exhibit complicated phenomena such as internal resonance, subharmonic resonance, etc… would be so readily described by the frequency-energy dependence of its NNMs as was shown here. Furthermore, the frequency content near each nonlinear mode of the structure seems to be consistent with what one would expect based on assuming that each nonlinear mode contains all of the energy present in the system. (Rather than, for example, each mode containing half of the energy in the system).
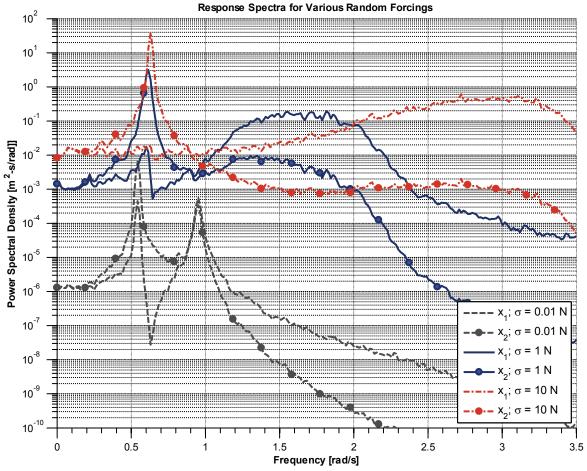

Figure 2. Power pectrum of the response of the 2DOF system at various forcing levels.

IV. Case Study – Clamped-Clamped Beam

A. Base Excitation Case

To explore these concepts further, the response of a clamped-clamped beam to random excitation was examined. The structure was modeled with 40 B31 beam elements in Abaqus® finite element software and has the physical properties listed in Table 1. This work first subjects the beam to a random base excitation, making this case identical to one that was studied by Gordon and Hollkamp in [1]. The excitation is a zero-mean Gaussian force with a standard deviation of 8g and a bandwidth of 0 to 2000 Hz.

Table 1: Physical properties of the clamped-clamped beam

Length	Width	Thickness	Young's Modulus	Shear Modulus	Mass Density
9 in	0.5 in	0.031 in	$2.97 \cdot 10^7$ psi	$1.16 \cdot 10^7$ psi	$7.36 \cdot 10^{-4} \ \dfrac{\text{lb} \cdot \text{s}^2}{\text{in}^4}$

It is quite expensive to compute the random response of the full finite element model, and reduced order models were also needed to more easily estimate its nonlinear modes, so several reduced order models were created and will be validated before proceeding. Due to the form of the excitation, only symmetric modes need be considered for inclusion in the ROM. The model itself is constructed using the ICE method [13], using cubic nonlinear terms only, with a scaling displacement of one beam thickness. This was found in [16] to give excellent predictions for the first several NNMs of the structure. The first three odd NNMs of the system are plotted in Figure 3 with comparisons between a single-mode ROM, four-mode ROM, and a truth model computed using the Applied Modal Force (AMF) algorithm in [15]. The AMF algorithm iteratively adjusts the initial conditions in the full finite element model until a periodic response is identified, and hence the solutions that it obtains are true NNMs (to a certain tolerance) of the finite element model.

The single-mode curves track well at low energies; in [16], Allen et al. found that an ICE ROM such as those used here usually predicted the backbone of the true NNM quite accurately (as is the case here), even when only one mode was included in the ROM. At high enough energies, however, the single-mode curve does begin to trend upwards more quickly than the four-mode and AMF curves. (While most easily seen in Figure 3a, the same trend is realized in the 3rd and 5th NNMs.) This corresponds to a stiffer system in which the frequency increases to a greater extent with increasing deflection. Adding modes to the ROM softens the system, resulting in a curve almost indistinguishable from the AMF model.

Since each of the single-mode ROMs accurately captures the response of a single nonlinear mode, they can be used to probe the degree to which the response of the system can be predicted (or, more likely, cannot be predicted) using linear superposition of the nonlinear normal modes. This will be explored in the results that follow.

Internal resonances are also present in the system, with tongues in the 1st NNM backbone curve observable at 88 and 125 Hz in the mode [1,3,5,7] ROM. (The AMF algorithm was intentionally set to skip over the internal resonances, to avoid the computational expense required to compute them. In [15] a solution is shown which includes the internal resonances and they do agree well with those predicted by the ROM in Figure 3.)

Because this model is relatively simple, it was possible to integrate the full order finite element model of this beam within Abaqus. While modal damping is convenient to use within the ROM formulation, the ABAQUS software does not allow one to define modal damping ratios to be used in a nonlinear transient simulation. Hence, mass and stiffness proportional damping with $[\mathbf{C}] = \alpha [\mathbf{M}] + \beta [\mathbf{K}]$, was used instead in the full-order model. In [1], it was noted that the damping ratios of the first two symmetric modes were experimentally observed to be $\zeta_1 = 0.3\%$ and $\zeta_3 = 0.5\%$. To maintain comparable values over the 2000 Hz frequency range of interest, these damping ratios were imposed at frequencies of 78 Hz and 2000 Hz. Damping factors of $\alpha = 4.77$ and $\beta = 7.77 \cdot 10^{-7}$ were necessary to fulfill this requirement.
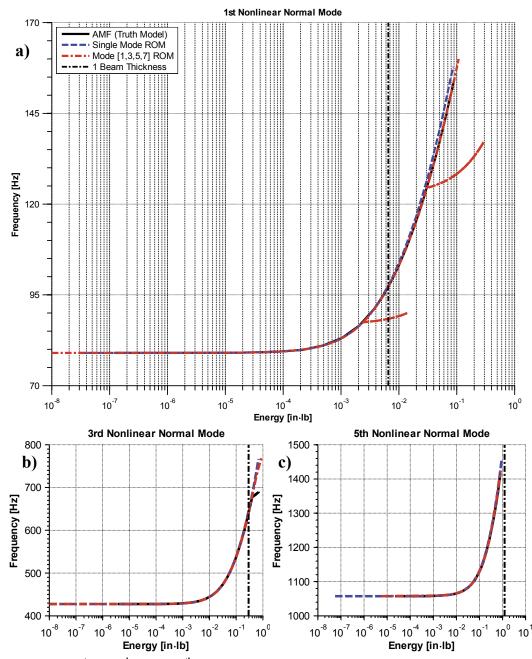
Figure 3. (a) 1ˢᵗ, (b) 3ʳᵈ, and (c) 5ᵗʰ NNMs of the clamped-clamped beam. Vertical line indicates the potential energy associated with a one beam-thickness deflection in each NNM.

MATLAB® was used to define the amplitude of the random load at each node in the finite element model at a fixed time-step. Based on the results of a convergence study, a sample rate of 50 kHz was chosen; this sample rate also corresponded to the step size used within the finite element integrator. To obtain statistically significant results, a relatively long time history was required; a 25 second simulation was used which yielded 1,250,000 time points. This took roughly 12 hours to integrate on a 3.4 GHz Intel® Core i7 with 12 GB of RAM. To examine the system's behavior when represented by reduced order models, the Newmark integration method was implemented within MATLAB and used with the same loading conditions supplied to the Abaqus integration above, to determine the response of the reduced order models to the excitation. The most accurate of these, the 4-mode ROM containing modes 1, 3, 5, and 7, was used to compute the beam's energy distribution over the integration period. A histogram of the instantaneous energy levels was normalized against the total number of time samples to create a probability mass function (PMF) giving the discrete probabilities of each energy value; this is shown with gray dots in Figure 4.
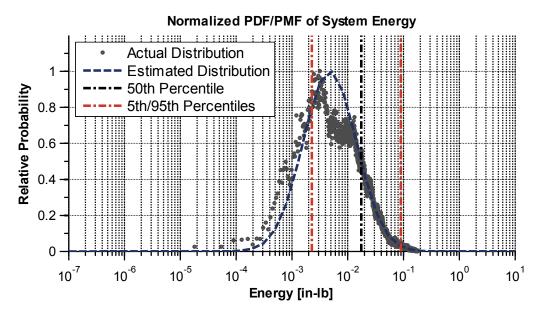
Normalized PDF/PMF of System Energy

Figure 4. Actual and estimated energy distributions for the 8*g* base excitation.

As was the case with the two-degree-of-freedom system above, the distribution resembles a bell curve on a logarithmic scale, so it may be approximated as a log-normal distribution. The resulting curve, along with its 5th, 50th and 95th percentile energy levels, are also plotted in Figure 4.

The power spectral density (PSD) response spectra of the various models are displayed in Figure 5. The spectrum of the truth model, obtained by integrating the full finite element model, is shown in each subplot with a solid black line. Figure 5a displays the response of a ROM that contained modes 1, 3, 5 and 7 compared to the response of the full-order system as described above. Figure 5b compares the response of single-mode models for modes 1, 3, and 5 with the truth model, while Figure 5c does the same for two-mode reduced order models using different pairs of modes. Before comparing the levels of accuracy inherent in each model, it is interesting to consult the frequency-energy plots from Figure 3 and energy distribution from Figure 4 to see whether the degree of peak smearing can be predicted by referencing each NNM's frequency at the energy percentiles plotted above. The vertical lines in Figure 5a show this comparison for each NNM. The center of each peak lies near the 50th percentile marker, while the distribution of each peak is found to be bracketed by the 5th and 95th percentile frequencies. While no physically significant measure (i.e., the half-power bandwidth of the peak) seems associated with these frequency values, the illustration does support the concept that one can estimate how much an NNM's frequency shifts from random excitation by simply assuming that all of the energy present in the system is in that mode and then reading the bounds off of a plot of the corresponding nonlinear normal mode. (In other words, taking no effort to apportion the energy among the different active modes.)

On the other hand, the situation changes if each mode is considered in isolation. In this case, the ROM that captures each NNM was integrated with the same applied force (so the energy in each NNM was different than in the previous case). Figure 5b shows that the mode 1 ROM model predicts the response near the first peak very well, while the mode 3 and mode 5 ROMs predict a peak that is far too sharp (the nonlinearity is not strong enough). This illustrates a case where the response of the system cannot be predicted by linearly super-imposing the response of individual ROMs (or, by extension, of individual nonlinear modes). The authors investigated this result and found that it could be explained using a set of linear single-degree-of-freedom models. Suppose that the structure was deformed statically into its first mode of vibration with large amplitude and then the 3rd and 5th natural frequencies were computed about that deformed state. The deformation induces tension in the beam which increases (stiffens) the 3rd and 5th natural frequencies somewhat. The authors studied this hypothesis quantitatively by using the mode-1 ROM solution to determine the displacement of the beam at every instant in time and computing the frequencies of modes 3 and 5 when linearized about that state. The distribution of the mode 3 and 5 frequencies was then estimated over the time record and it was found to predict the width of the PSD near modes 3 and 5 very accurately. That calculation is shown in the Appendix. This discussion illustrates that although linear superposition does not hold for a nonlinear system, the modes still can be useful in understanding the spectrum of the response.
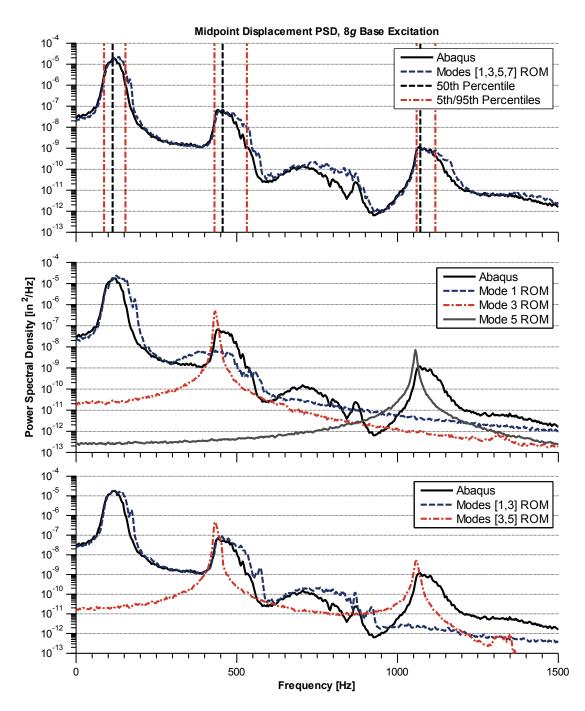
American Institute of Aeronautics and Astronautics

Figure 5. Power spectral density estimates for various ROMs compared to the Abaqus truth model. (a) Four-mode ROM, (b), Single-mode ROMs, (c), Two-mode ROMs.

The discussion in the previous paragraph can be summarized by simply observing that for this system and loading condition, any ROM must include the first mode and coupling between other modes and that mode, in order to accurately predict the response. This is illustrated in Fig. 5c, where two pairs of modes were used to create ROMs and the response was computed. The first of these models contained modes 1 and 3, the second contained modes 3 and 5. It is clear that, when mode 1 was included, the response of both modes 1 and 3 was accurate. While not shown, a ROM containing modes 1 and 5 behaves in a similar manner. These results suggest that, while a mode must be included in the ROM in order to obtain the corresponding response peak, the response as a whole may be inaccurate if a particular dominant mode is left out. In this case, mode 1 is dominant, due to the form of the

excitation, so its effect on the structure must be considered to correctly predict the response even at frequencies that are significantly higher.

B. Random Pressure Field Excitation

In the applications of interest, structures are excited by a random pressure field, so one further load case was considered to see the effect of a more general loading. Here, a forcing was used that is a random function of both position and time. A correlation matrix is defined such that,

$$E[\mathbf{y}\mathbf{y}^T] = \mathbf{C} \quad where \quad C_{ij} = \exp[-\alpha \mid x_i - x_j \mid] \tag{11}$$

with $E[]$ the expected value operator, α a positive constant and $\mid x_i - x_j \mid$ the distance between the ith and jth points. In the continuous sense, $\mathbf{y}$ is a vector of correlated random forcing functions, with each random element corresponding to a nodal force. To implement this field it is convenient to create a matrix $\mathbf{Y}$ which has a column for each time instant. If the model contains q nodes and is simulated at r time steps, $\mathbf{Y}$ has dimension $q \times r$. To find this correlated random field, one first obtains the lower triangular Cholesky decomposition of $\mathbf{C}$, denoted as $\mathbf{b}$, so that $\mathbf{C} = \mathbf{b}^T\mathbf{b}$. Then, given a matrix $\mathbf{W}$ of q independent variables at r time steps, the random time history can then be found using the following.

$$\mathbf{Y} = \mathbf{bW} \tag{12}$$

In the case that follows, the initial random matrix $\mathbf{W}$ consisted of independent, Gaussian random variables with zero mean and standard deviations of 0.08 lb. The 25 second time histories were sampled at 50 kHz and filtered through an 8th order low-pass Butterworth filter with a critical frequency of 2000 Hz. A correlation constant of $\alpha = 0.5$ was used to obtain the correlation matrix. In this manner, the set of initially independent vectors were "smoothed" across the beam, to provide a forcing reminiscent of physically realizable loadings. Due to the asymmetric nature of this loading scenario, both even and odd linear modes were excited and will be used in the construction of the ROMs for this case.

As above, the energy distributions were first determined and are shown in Figure 6. For this case, the distribution was computed using a ROM that contained modes one through four. (The second and fourth NNMs, though not shown, had converged to the AMF solution.)
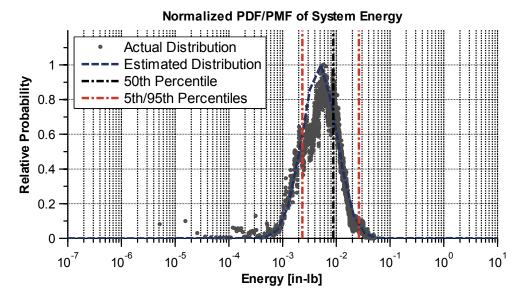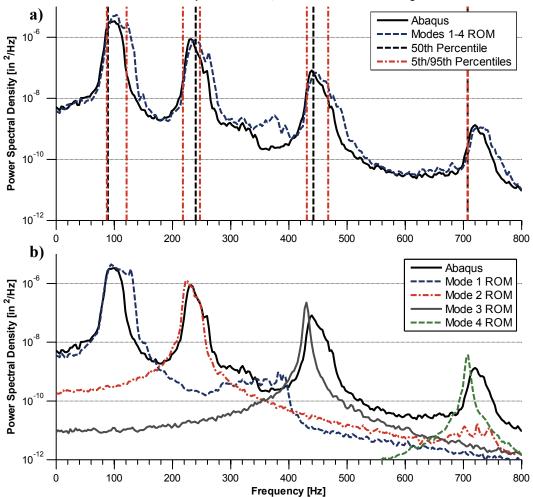

Figure 6. Actual and estimated distributions for the energy distribution of the correlated excitation

Figure **7** shows the beam's response to this excitation, as simulated using a full order model and a variety of reduced order models: A ROM with modes 1 through 4, as well as the first four single-mode models, is plotted along with the full-order solution. Since the forcing is no longer symmetric, it is the power spectral density of the node at x = L/3 that is shown, allowing examination of asymmetric modes.

As in the previous example, the distribution of energy and the NNM curves were used to predict the width of each resonance peak, and the predicted widths (vertical lines) are compared with the actual spectrum in Figure **7**a. Two interesting points are immediately of note. The first NNM's 50th percentile frequency is almost identical to that of its 5th percentile frequency, leading to an asymmetric bracket for the mode. More significantly, while the bounds give a reasonable estimate of the width of the peaks in the spectrum for modes 1-3, the fourth NNM was not predicted to exit the linear regime to any extent, and yet the response near the 4th mode shows significant smearing. While the erroneous prediction for this mode could, perhaps, be explained as in the previous sections, it is clear that superposition does not hold for this mode.

Examining the accuracies of the various ROMs, we first observe that the modes 1-4 ROM is less accurate for this excitation than the modes [1,3,5,7] ROM in the previous case. The modes 1-4 ROM is able to locate the response peaks accurately, yet the peak spread is over-predicted somewhat, indicating that the ROM is too stiff. This is, perhaps, to be expected, as the mode [1,3,5,7] ROM included all relevant modes out to 1500 Hz while the mode 1-4 ROM only captures modes to 800 Hz.

Several one-mode models were also used to predict the corresponding part of the response spectrum. In the previous case, mode one was clearly dominant, while in this case modes one and two have about equal strength. The results show that modes one and two could each be used alone to predict the corresponding part of the spectrum, revealing that these modes are not nonlinearly coupled. Examining the ROMs created with modes three and four, it is apparent that these modes were more readily excited by the correlated forcing. As a result, the 2nd and 3rd mode ROMs exhibit some nonlinear behavior, although their peaks are not smeared to the extent seen in the truth model.

Figure 7. Power spectral density comparisons of full and reduced-order models using a random forcing correlated with position. (a) Four-mode ROM. (b) Single-mode ROMs.

American Institute of Aeronautics and Astronautics

V. Conclusions

This work has explored the connection between the random response of a structure and its undamped nonlinear normal modes. Simulations illustrated that the response to random input of each mode of the nonlinear structure is smeared over a range of frequencies when the excitation force is large, as expected due to the stiffening effect of the geometric nonlinearity. Furthermore, for the examples studied here, the degree of spreading in the power spectrum could be quantitatively predicted using the frequency-energy plot. At a given excitation level, if the energy in the structure spread over a range where the NNM frequencies varied significantly, the power spectrum would broaden in a commensurate manner. However, several exceptions to this oversimplified thinking were noted and should be kept in mind. The exceptions arise because the nonlinear modes are not uncoupled as linear modes are, so they generally cannot be considered in isolation. Even then, the response of the geometrically nonlinear beam studied here was dominated by one or two modes and hence one could predict the overall response quite accurately considering only one mode, and this may be a common occurrence in practice.

The authors believe that the more important finding here is just how intimately connected a structure's nonlinear normal modes are to its forced, random response. Hence, if a reduced order model is capable of accurately predicting the frequency-energy backbone of the nonlinear modes in the frequency-energy range of interest, then the results presented here suggest that it will also accurately predict the random response of a nonlinear structure in that same range of frequency and energy. While this claim cannot be proven generally, it seems reasonable if one considers that nonlinear modes are solutions of the equations of motion or, equivalently, surfaces in the state space which are tangent to the vector field. If those points of tangency are accurately captured by a reduced model then it certainly seems reasonable that the model should accurately predict the response to a random input. On the other hand, this work has only considered the primary NNM branches, neglecting the internal resonances and other period lengthened solutions such as those shown in [6]. Those branches of solutions also define invariant paths in the state space and it is not yet clear whether a reduced order model must capture all of these other solutions to accurately predict the structure's response.

One may question whether it is advantageous to validate a reduced order model using NNMs rather than its PSDs. On the one hand, the PSD is a physical quantity which is more meaningful for design, and it has been used previously to validate models (see, e.g. [1]). On the other hand, the PSD depends on response amplitude so the comparison must be performed with various loading scenarios and monitoring the response at many points. In contrast, the NNMs are deterministic and they may be less expensive to compute over a range of energy than a PSD. The NNMs are also a global property of the structure, so if the relevant NNMs are accurate then one can be assured that the responses anywhere on the structure are also accurate and one can readily visualize the deformation of the whole structure in terms of its NNMs. The NNMs are also independent of the shape of the random input and one NNM captures the response at a large range of excitation levels.

These findings can be used to dramatically reduce the computation required to predict the random response of the geometrically nonlinear skin panels that are of interest in this work. In the applications of interest it is not practical to integrate the nonlinear finite element model to obtain truth data; indeed, this took 12 hours even for simple finite element model used here, which had only 117 DOF! In contrast, one-mode reduced order models can be readily computed for most structures of interest and ROMs with a small number of modes are also within reach. The random response of those ROMs is then relatively inexpensive to compute (1-2 minutes or less).

Acknowledgments

Appendix

An examination of mode 1's effect on the frequency shift and spread of higher modes was conducted. Qualitatively, this effect is a result of the stiffening behavior generated by a deflection in mode 1; it was postulated that, since mode 1 was dominant in the responses studied, the nonlinearity seen in the frequency response of higher modes was dependent on this mode. To accomplish this goal, the undamped free response was first considered. An alternative formulation of a reduced order model containing m modes is given by Nash [16],

$$\mathbf{I}_m \ddot{\mathbf{q}} + [\mathbf{\Lambda}_m + \frac{1}{2}\mathbf{N}_1(\mathbf{q}) + \frac{1}{3}\mathbf{N}_2(\mathbf{q})]\mathbf{q} = \mathbf{0} \tag{A1}$$

Where $\mathbf{I}_m$ is the identity matrix of order m and $\mathbf{\Lambda}_m$ contains the squared natural frequencies of each included mode along its diagonal. $\mathbf{N}_1(\mathbf{q})$ and $\mathbf{N}_2(\mathbf{q})$ are $m \times m$ nonlinear stiffness matrices which correspond to quadratic and cubic nonlinearities, respectively. Defining these matrices is a two-step process. First, a vector of cubic terms must be constructed. (The quadratic terms, while not used for this structure, can treated in a similar manner).

$$\mathbf{\alpha} = [\alpha_1 \quad \alpha_2 \quad ... \quad \alpha_m]^T \quad where \quad \alpha_i = \sum_{i=1}^{m}\sum_{j=1}^{m}\sum_{k=1}^{m} A_i(i,j,k)q_i q_j q_k \tag{A2}$$

The nonlinear stiffness matrix is then the Jacobian matrix of $\mathbf{\alpha}$ with respect to $\mathbf{q}$.

$$\mathbf{N}_2(\mathbf{q}) = \frac{\partial \mathbf{\alpha}}{\partial \mathbf{q}} \tag{A3}$$

If the postulate above holds, then approximating the system as linear near a particular deflection of the first mode should be valid. This is accomplished by formulating an equivalent linear stiffness about a particular deflection state of mode 1, $\mathbf{q}_0 = [q_1 \quad 0 \quad ... \quad 0]^T$.

$$\mathbf{K}_{eq} = \left(\frac{\partial}{\partial \mathbf{q}}[\mathbf{\Lambda}_m + \frac{1}{2}\mathbf{N}_1(\mathbf{q}) + \frac{1}{3}\mathbf{N}_2(\mathbf{q})]\mathbf{q} \right)_{\mathbf{q}=\mathbf{q}_0} \tag{A4}$$

Equation (A1) can now be written as a linear system, from which the modified natural frequencies can be extracted by solving the general eigenvalue problem,

$$\mathbf{I}_m \ddot{\mathbf{q}} + \mathbf{K}_{eq}\mathbf{q} = \mathbf{0} \tag{A5}$$

In this manner, the dependence of frequency on displacement can be easily approximated for responses in which a single mode is dominant, by applying the statistics of a known single-mode response to a higher-order ROM. To examine the effectiveness of these distributions, the mean and standard deviations can be estimated and compared to the measured response. For both loading cases tested in this work, each mode's mean frequency was an excellent approximation to the nonlinear response peak, and the standard deviation of each mode served as a useful measure of the width of each response peak. As an example, if the mode 1 response distribution in Figure 7 is applied to a ROM containing modes 1, 2, 3, and 4, a probability distribution function of each mode's modified natural frequency can be constructed. The estimated response peak locations and corresponding widths are shown in Figure A1. The mode 3 and mode 4 peaks are well-approximated by this linearization method, while the 2nd mode peak location is underestimated to some extent. This indicates that the nonlinearity in modes 3 and 4 are completely dependent on that caused by mode 1 deflections, while mode 2's actual response is somewhat less dependent on the deflection level of mode 1.
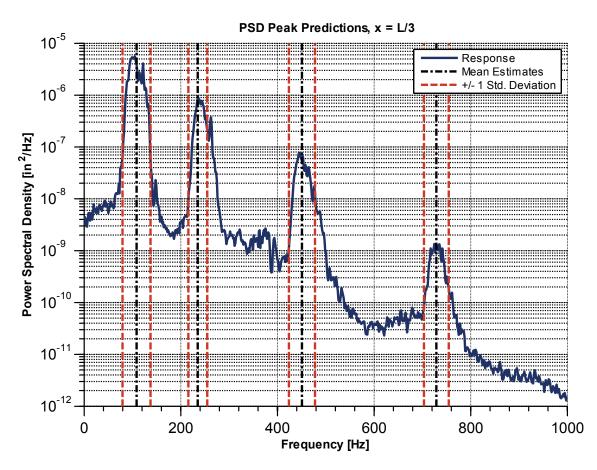
PSD Peak Predictions, x = L/3

Figure A1. Peak prediction brackets obtained via linearizing the stiffness matrix about mode 1's instantaneous deflection

References

[1]   R. W. Gordon and J. J. Hollkamp, "Reduced-order Models for Acoustic Response Prediction," Air Force Research Laboratory, Dayton, OH2011.

[2]   R. M. Rosenberg, "Normal modes of nonlinear dual-mode systems," *Journal of Applied Mechanics,* vol. 27, pp. 263–268, 1960.

[3]   G. Kerschen, M. Peeters, J. C. Golinval, and A. F. Vakakis, "Nonlinear normal modes. Part I. A useful framework for the structural dynamicist," *Mechanical Systems and Signal Processing,* vol. 23, pp. 170-94, 2009.

[4]   A. F. Vakakis, "Non-linear normal modes (NNMs) and their applications in vibration theory: an overview," *Mechanical Systems and Signal Processing,* vol. 11, pp. 3-22, 1997.

[5]   H. A. Ardeh and M. S. Allen, "Instantaneous Center Manifolds and Nonlinear Modes of Vibration," presented at the ASME 2012 International Design Engineering Technical Conferences, Chicago, IL, 2012.

[6]   H. A. Ardeh and M. S. Allen, "Investigating Cases of Jump Phenomenon in a Nonlinear Oscillatory System," presented at the 31st International Modal Analysis Conference (IMAC XXXI), Garden Grove, CA, 2013.

[7]   B. K. Øksendal, *Stochastic Differential Equations: An Introduction with Applications.* Berlin: Springer, 2003.

[8]   D. A. W. Barton, S. G. Burrow, and L. R. Clare, "Energy Harvesting From Vibrations With a Nonlinear Oscillator," *Journal of Vibration and Acoustics,* vol. 132, p. 021009 (7 pp.), 2010.

[9]   P. Kumar and S. Narayanan, "Modified path integral solution of Fokker-Planck equation: response and bifurcation of nonlinear systems," *Journal of Computational and Nonlinear Dynamics,* vol. 5, p. 011004 (12 pp.), 2010.

[10]   E. J. Cross and K. Worden, "Approximation of the Duffing oscillator frequency response function using the FPK equation," *Journal of Physics: Conference Series,* vol. 181, p. 012085 (9 pp.), 2009.

[11]   M. Peeters, G. Kerschen, and J. C. Golinval, "Dynamic testing of nonlinear vibrating structures using nonlinear normal modes," *Journal of Sound and Vibration,* vol. 330, pp. 486-509, 2010.

[12]   R. J. Kuether and M. S. Allen, "Computing Nonlinear Normal Modes Using Numerical Continuation and Force Appropriation," presented at the ASME 2012 International Design Engineering Technical Conferences IDETC/CIE 2012, Chicago, IL, 2012.

[13]   J. J. Hollkamp and R. W. Gordon, "Reduced-order models for nonlinear response prediction: Implicit condensation and expansion," *Journal of Sound and Vibration,* vol. 318, pp. 1139-1153, 2008.

[14]   M. Peeters, R. Viguie, G. Serandour, G. Kerschen, and J. C. Golinval, "Nonlinear normal modes, part II: toward a practical computation using numerical continuation techniques," *Mechanical Systems and Signal Processing,* vol. 23, pp. 195-216, 2009.

[15]   R. J. Kuether and M. S. Allen, "A Numerical Approach to Directly Compute Nonlinear Normal Modes of Geometrically Nonlinear Finite Element Models," *Mechanical Systems and Signal Processing,* vol. Submitted, 2013.

[16]   M. S. Allen, R. J. Kuether, B. Deaner, and M. W. Sracic, "A Numerical Continuation Method to Compute Nonlinear Normal Modes Using Modal Reduction," presented at the 53rd AIAA Structures, Structural Dynamics, and Materials Conference, Honolulu, Hawaii, 2012.

[17]   M. S. Allen and R. J. Kuether, "Substructuring with Nonlinear Subcomponents: A Nonlinear Normal Mode Perspective," presented at the 30th International Modal Analysis Conference, Jacksonville, Florida, 2012.